

Shape-from-Operator: Recovering Shapes from Intrinsic Operators

Davide Boscaini, Davide Eynard, Drosos Kourounis, and Michael M. Bronstein

Faculty of Informatics, Università della Svizzera italiana (USI), Lugano, Switzerland

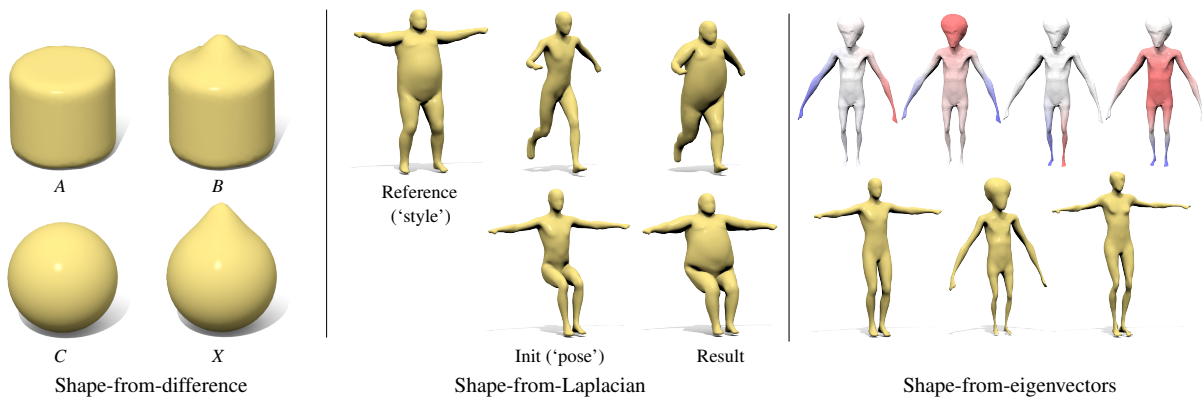


Figure 1: Examples of three different shape-from-operator problems considered in the paper. Left: shape analogy synthesis as shape-from-difference operator problem (shape X is synthesized such that the intrinsic difference operator between C, X is as close as possible to the difference between A, B). Center: style transfer as shape-from-Laplacian problem. The Laplacian of the leftmost shape (fat man) captures the style, while the initial thin man shape (middle) captures the pose. Right: we deform the human shape (bottom leftmost) such that its Laplacian is diagonalized by the first 10 eigenfunctions of the alien Laplacian (top row). The result (bottom rightmost) is an ‘intrinsic hybrid’ between the two shapes.

Abstract

We formulate the problem of shape-from-operator (SfO), recovering an embedding of a mesh from intrinsic operators defined through the discrete metric (edge lengths). Particularly interesting instances of our SfO problem include: shape-from-Laplacian, allowing to transfer style between shapes; shape-from-difference operator, used to synthesize shape analogies; and shape-from-eigenvectors, allowing to generate ‘intrinsic averages’ of shape collections. Numerically, we approach the SfO problem by splitting it into two optimization sub-problems: metric-from-operator (reconstruction of the discrete metric from the intrinsic operator) and embedding-from-metric (finding a shape embedding that would realize a given metric, a setting of the multidimensional scaling problem). We study numerical properties of our problem, exemplify it on several applications, and discuss its limitations.

Categories and Subject Descriptors (according to ACM CCS): Computer graphics [I.3]: Shape modeling—Shape analysis

1. Introduction

Everyone who has done an IQ test would have seen geometric shape analogy [BO00] problems, in which one is shown three shapes: source A , target B , and exemplar C . The test subject’s goal is to produce a shape X such that the same

relation (analogy) holds between C and X as between A and B . For example, given a sphere and a bumped sphere as the source and the target, and a cylinder as the exemplar, one expects to see a bumped cylinder as the shape analogy (Figure 1, left). Rustamov et al. [ROA*13] proposed modeling

shape relations by intrinsic linear operators, which allows one to tell in a convenient way not only how intrinsically different two shapes are, but also where and in which way they differ. Roughly speaking, such a shape difference operator defines the notion of ' $B - A$ ' for shapes. The shapes C, X are analogous to A, B if ' $B - A = X - C$ '.

The problem of finding a shape analogy ' $X = C + (B - A)$ ' boils down to reconstructing a shape from an intrinsic shape difference operator. This is just a particular setting of what we term a *shape-from-operator* (SfO) problem: shape reconstruction from intrinsic operators, such as Laplacians or the aforementioned shape difference operators. Here, we interpret ‘shape reconstruction’ as finding an embedding of the shape in the 3D space inducing a Riemannian metric, that, in turn, induces intrinsic operators with desired properties. For example, in the *shape-from-Laplacian problem* (Figure 1, center), we try to deform a shape in such a way that the Laplacian operator of the new shape matches some given ‘reference’ Laplacian.

Main contributions In this paper, we formulate the general *shape-from-operator* (SfO) problem and study a few interesting instances thereof. Numerically, we approach the SfO problem by splitting it into two optimization sub-problems: metric-from-operator (reconstruction of the Riemannian metric from the intrinsic operator, which, in the case of shapes discretized as triangular meshes, is represented by edge lengths) and shape-from-metric (finding a shape embedding that would realize a given metric). As particular cases of our approach, we show applications of *shape-from-Laplacian* for style/deformation transfer, *shape-from-difference* for the synthetization of shape analogies, and *shape-from-eigenvectors* for the generation of ‘intrinsic averages’ of shape collections.

The rest of the paper is organized as follows. In Section 2, we overview some of the related works. Section 3 introduces the notation and mathematical setting of our problem. In Section 4 we formulate the shape-from-operator problem, and consider several particular settings thereof. We also discuss a numerical optimization scheme for solving this problem. Section 5 provides experimental validation of the proposed approach. We study the numerical properties of our problem and show examples of shape reconstruction from Laplacian, eigenvectors, shape analogy synthesis, and shape caricaturization. Limitations and failure cases are discussed in Section 6, which concludes the paper.

2. Related work

Shape reconstruction problems have been a topic of intensive research in computer vision, graphics, and geometry processing for several decades. Classical examples include shape-from-motion [Kan85], shading [IH81], photometric stereo [Woo80], as well as more exotic examples such as texture [Ike84], contour [Wit80] and sketches [KH06].

In the context of geometry processing, shape reconstruction from intrinsic structures such as metric or curvature has

numerous applications including parametrization and texture mapping (see, e.g. [IGG01, SdS01, BCGB08, KG08, CPS11, WLT12, PPTSH14]). Multidimensional scaling (MDS) problems [BG05] try to find a configuration of points in the Euclidean space that realize some given distance structure.

Recently, there has been interest in metric reconstruction from the Laplacian. A well-known fact in differential geometry is that the Laplace-Beltrami operator is fully determined by the Riemannian metric [Ros97], and, conversely, the metric is determined by the Laplace-Beltrami operator (or a heat kernel constructed from it) [ZGLG12]. In the discrete setting, the length of edges of a triangular mesh plays the role of the metric, and fully determines the discrete Laplacian. Zeng et al. [ZGLG12] showed that the converse also holds for discrete metrics, and formulated the problem of discrete metric reconstruction from the Laplacian. It was shown later by [dGMMD14] that this problem boils down to minimizing the conformal energy.

Our shape-from-operator problem can be viewed as a natural continuation of these works. The metric-from-operator part of the SfO problem is an extension of [ZGLG12, dGMMD14], as we consider more generic intrinsic operators that include Laplacians as particular examples and remove the assumption of initial and reference shape having vertex-wise bijective correspondence. MDS problems can be regarded as problems of shape-from-metric reconstruction, which is the second part of the SfO problem: recover the embedding given the metric found as the solution to the metric-from-operator problem.

We rely on the recent works on operator-based approaches to geometric processing and analysis problems such as correspondence [OBCS^{*}12], signal processing on manifolds [ABCCO13], and quantifying differences between shapes [ROA^{*}13]. Our approach is also related to recent works in machine learning [BGL13] and image processing [EKMB14] communities, where the authors try to modify graph Laplacians in order to satisfy certain properties such as commutativity. In our case, we have meshes instead of graphs and more generic operators; we try to modify the operator (parametrized through the metric) to make it satisfy some problem-dependent properties, and then find an embedding that realizes this metric.

Finally, several applications we use to exemplify our problem have been considered from other perspectives. In particular, methods for shape deformation, pose transfer, and editing have been proposed by [SP04, SCOL^{*}04, LSLCO05, RCG08, BVGP09]. 2D and 3D shape analogies were studied in [HJO^{*}01, ROA^{*}13, MHS^{*}14]. Analysis and transfer of shape style have been presented by [XLZ^{*}10, WBAL11, MWZ^{*}13, MHS^{*}14, ALX^{*}14]. Finally, shape exaggeration and caricaturization have been studied in [LVM^{*}11, CCM11].

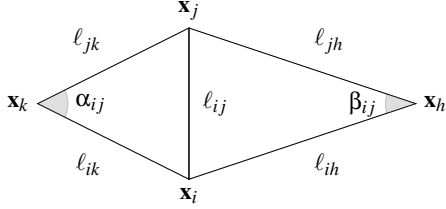


Figure 2: Notation used in the paper: edge ij has length ℓ_{ij} . Angles α_{ij} and β_{ij} are opposite to edge ij . Triangle ijk has area A_{ijk} .

3. Background

3.1. Basic definitions

Throughout the paper, we denote by $\mathbf{A} = (a_{ij})$, $\mathbf{a} = (a_i)$, and a real matrices, vectors, and scalars, respectively. $\|\mathbf{A}\|_F = \sqrt{\sum_{ij} a_{ij}^2}$ denotes the Frobenius norm of a matrix. We model a 3D shape as a connected smooth compact two-dimensional surface X without boundary, and tacitly assume that all the surfaces have fixed topology, e.g. genus zero. We denote by $T_x X$ the tangent space at point x and define the Riemannian metric as the inner product $\langle \cdot, \cdot \rangle_{T_x X} : T_x X \times T_x X \rightarrow \mathbb{R}$ on the tangent space. We denote by $L^2(X)$ the space of square-integrable functions and by $H^1(X)$ the Sobolev space of weakly differentiable functions on X modulo constants. We then define the standard inner products on these spaces as

$$\langle f, g \rangle_{L^2(X)} = \int_X f(x)g(x)da(x); \quad (1)$$

$$\langle f, g \rangle_{H^1(X)} = \int_X \langle \nabla f(x), \nabla g(x) \rangle_{T_x X} da(x) \quad (2)$$

where da denotes the area element induced by the Riemannian metric. The *Laplace-Beltrami operator* Δf is defined through the *Stokes formula*, $\langle \Delta f, g \rangle_{L^2(X)} = \langle f, g \rangle_{H^1(X)}$, and is *intrinsic*, i.e., expressible entirely in terms of the Riemannian metric (as opposed to *extrinsic* properties depending on the embedding).

3.2. Discrete metrics and Laplacians

In the discrete setting, the surface X is approximated by a manifold triangular mesh (V, E, F) with vertices $V = \{1, \dots, n\}$, in which each edge $ij \in E$ is shared by exactly two triangular faces (ijk and $jhi \in F$; see Figure 2 for this and the following definitions). A real function $f : X \rightarrow \mathbb{R}$ on the surface is sampled on the vertices of the mesh and can be identified with an n -dimensional vector $\mathbf{f} = (f_1, \dots, f_n)^\top$. A discrete Riemannian metric is defined by assigning each edge ij a length $\ell_{ij} > 0$, satisfying the strong triangle inequality[†],

$$\ell_{ij} + \ell_{jk} - \ell_{ki} > 0, \ell_{jk} + \ell_{ki} - \ell_{ij} > 0, \ell_{ki} + \ell_{ij} - \ell_{jk} > 0, \quad (3)$$

for all $i, j, k : ijk \in F$. We denote by $\boldsymbol{\ell} = (\ell_{ij} : ij \in E)$ the vector of edge lengths of size $|E|$, representing the discrete metric.

[†] We require a strong version of the triangle inequality to avoid zero-area triangles.

The inner product on piecewise constant functions associated with barycentric dual cells is discretized as $\langle \mathbf{f}, \mathbf{g} \rangle_{L^2(X)} = \mathbf{f}^\top \mathbf{Ag}$, where $\mathbf{A} = \text{diag}(a_1, \dots, a_n)$ and $a_i = \frac{1}{3} \sum_{j:ijk \in F} A_{ijk}$ is the local area element at vertex i ; A_{ijk} denotes the area of triangle ijk . Using Heron's formula for triangle area, we can express

$$A_{ijk} = \sqrt{s(s - \ell_{ik})(s - \ell_{kj})(s - \ell_{ij})}, \quad (4)$$

$$s = (\ell_{ik} + \ell_{kj} + \ell_{ij})/2,$$

entirely in terms of the discrete metric.

The discrete version of the Laplace-Beltrami operator is given as an $n \times n$ matrix $\mathbf{L} = \mathbf{A}^{-1} \mathbf{W}$, where \mathbf{W} is the *stiffness matrix*

$$w_{ij}(\boldsymbol{\ell}) = \begin{cases} \frac{-\ell_{ij}^2 + \ell_{jk}^2 + \ell_{ki}^2}{8A_{ijk}} + \frac{-\ell_{ij}^2 + \ell_{jh}^2 + \ell_{hi}^2}{8A_{ijh}} & ij \in E; \\ -\sum_{k \neq i} w_{ik} & i = j; \\ 0 & \text{else.} \end{cases} \quad (5)$$

Such a matrix is positive semi-definite and has a zero eigenvalue corresponding to a constant eigenvector. Note that since (5) is expressed entirely in terms of the edge lengths $\boldsymbol{\ell}$, the Laplacian $\mathbf{L}(\boldsymbol{\ell}) = \mathbf{A}(\boldsymbol{\ell})^{-1} \mathbf{W}(\boldsymbol{\ell})$ is intrinsic [JS12].

An *embedding* is the geometric realization of the mesh (V, E, F) in \mathbb{R}^3 specified by providing the three-dimensional coordinates \mathbf{x}_i for each vertex $i \in V$ (we will hereinafter represent the embedding by an $n \times 3$ matrix \mathbf{X}). Such an embedding induces a metric $\boldsymbol{\ell}(\mathbf{X}) = (\|\mathbf{x}_i - \mathbf{x}_j\| : ij \in E)$. With this metric, it is easy to verify that formula (5) becomes the standard cotangent weight [PP93, MDSB03]

$$w_{ij} = \begin{cases} (\cot \alpha_{ij} + \cot \beta_{ij})/2 & ij \in E; \\ -\sum_{k \neq i} w_{ik} & i = j; \\ 0 & \text{else,} \end{cases} \quad (6)$$

since $\cot \alpha_{ij} = \frac{-\ell_{ij}^2 + \ell_{jk}^2 + \ell_{ki}^2}{4A_{ijk}}$. Thus, an embedding \mathbf{X} defines a discrete metric $\boldsymbol{\ell}(\mathbf{X})$, and consequently, a discrete Laplacian $\mathbf{L}(\boldsymbol{\ell}(\mathbf{X}))$.

3.3. Metric-from-Laplacian

Zeng et al. [ZGLG12] showed that the cotangent Laplacian and the discrete Riemannian metric (unique up to a scaling) represented by edge lengths are defined by each other, and that the set of all discrete metrics that can be defined on a triangular mesh is convex. A discrete metric $\boldsymbol{\ell}$ that realizes a given ‘reference’ Laplacian can be found by minimizing the convex energy given implicitly by

$$\mathcal{E}_{\text{imp}}(\boldsymbol{\ell}) = \int_{\boldsymbol{\ell}_0}^{\boldsymbol{\ell}} \sum_{i,j} (\bar{w}_{ij} - w_{ij}(\boldsymbol{\ell})) d\ell_{ij} \quad (7)$$

where $w_{ij}(\boldsymbol{\ell})$ are the metric-dependent weights defined according to (5), $\boldsymbol{\ell}_0$ is the metric of a shape \mathbf{X}_0 used for initialization, and $\bar{\mathbf{W}} = (\bar{w}_{ij})$ is the stiffness matrix of the reference

Laplacian. De Goes et al. [dGMMD14] derived a closed-form expression of (7), which turns out to be the classical *conformal energy*

$$\mathcal{E}_{\text{conf}}(\boldsymbol{\ell}) = \frac{1}{2} \sum_{i,j} (w_{ij}(\boldsymbol{\ell}) - \bar{w}_{ij}) \ell_{ij}^2. \quad (8)$$

3.4. Functional correspondence

Ovsjanikov et al. [OBCS*12] proposed representing soft correspondences between shapes as operators between spaces of functions thereon. The correspondence between X and Y is modeled by a linear operator $F: L^2(X) \rightarrow L^2(Y)$ referred to as a *functional map*, which can be efficiently represented in the frequency domain, as follows. Denote by $\{\phi_p\}_{p \geq 1}$ the set of orthonormal eigenfunctions of the Laplace-Beltrami operator on X satisfying $\Delta_X \phi_p = \lambda_p \phi_p$, and similarly, by $\{\psi_q\}_{q \geq 1}$ the eigenfunctions of the Laplace-Beltrami operator on Y . Then, using Fourier expansion in these bases, one gets

$$\begin{aligned} Tf &= \sum_{p \geq 1} \langle f, \phi_p \rangle_{L^2(X)} \sum_{q \geq 1} \langle T\phi_p, \psi_q \rangle_{L^2(Y)} \psi_q \\ &= \sum_{p,q \geq 1} c_{pq} \langle f, \phi_p \rangle_{L^2(X)} \psi_q, \end{aligned} \quad (9)$$

where $c_{pq} = \langle T\phi_p, \psi_q \rangle_{L^2(Y)}$ are coefficients translating Fourier coefficients between the bases. Truncating the expansion at the first k basis vectors, one gets a $k \times k$ matrix of coefficients encoding the functional correspondence; the value of k determines the ‘quality’ of the approximation.

In the discrete setting, shapes X and Y are represented as triangular meshes with n and m vertices, respectively. The first k Laplacian eigenfunctions are represented by $n \times k$ and $m \times k$ matrices $\Phi = (\phi_1, \dots, \phi_k)$ and $\Psi = (\psi_1, \dots, \psi_k)$, respectively. Equation (9) can be re-written in matrix form as $\mathbf{F} = \Psi \mathbf{C}^\top \Phi^\top$. Ovsjanikov et al. [OBCS*12] showed that \mathbf{C} can be determined by providing a set of $r \geq k$ corresponding functions $\mathbf{P} = (\mathbf{p}_1, \dots, \mathbf{p}_r)$ and $\mathbf{S} = (\mathbf{s}_1, \dots, \mathbf{s}_r)$ on X and Y , respectively, by solving the linear system of equations

$$\mathbf{S}^\top \Psi = \mathbf{P}^\top \Phi \mathbf{C} \quad (10)$$

in the least-squares sense. Typically, intrinsic descriptors such as heat kernel signature (HKS) [SOG09] or stable regions [LBB11] are used as columns of matrices \mathbf{P}, \mathbf{S} , making the functional map \mathbf{F} intrinsic. In the following, we tacitly assume that all the functional maps are intrinsic.

3.5. Shape difference operators

Rustamov et al. [ROA*13] proposed representing the difference between shapes X and Y in the form of a linear operator on $L^2(X)$ describing how the respective inner products change under the functional map. Let $\langle \cdot, \cdot \rangle_X$ and $\langle \cdot, \cdot \rangle_Y$ denote some inner products on $L^2(X)$ and $L^2(Y)$, respectively. The *shape difference operator* is a unique self-adjoint linear operator $D_{X,Y}: L^2(X) \rightarrow L^2(X)$ satisfying

$$\langle f, D_{X,Y} g \rangle_X = \langle Ff, Fg \rangle_Y, \quad (11)$$

for all $f, g \in L^2(X)$. The shape difference operator depends on the choice of the inner products $\langle \cdot, \cdot \rangle_X$ and $\langle \cdot, \cdot \rangle_Y$. Rustamov et al. [ROA*13] considered the two inner products (1) and (2). The former gives rise to the *area-based* shape difference denoted by $V_{X,Y}$, while the latter results in the *conformal* shape difference $R_{X,Y}$ (see [ROA*13] for derivations and technical details).

In the discrete setting, the inner products are discretized as $\langle \mathbf{f}, \mathbf{g} \rangle_X = \mathbf{f}^\top \mathbf{H}_X \mathbf{g}$ and $\langle \mathbf{p}, \mathbf{q} \rangle_Y = \mathbf{p}^\top \mathbf{H}_Y \mathbf{q}$ (here \mathbf{H}_X and \mathbf{H}_Y are $n \times n$ and $m \times m$ positive-definite matrices, respectively). For the two aforementioned choices of inner products, the area-based difference operator is given by an $n \times n$ matrix

$$\mathbf{V}_{X,Y} = \mathbf{A}_X^{-1} \mathbf{F}^\top \mathbf{A}_Y \mathbf{F}, \quad (12)$$

where \mathbf{A} is matrix of area elements, and \mathbf{F} is the functional correspondence between X and Y . The conformal shape difference operator is

$$\mathbf{R}_{X,Y} = \mathbf{W}_X^\dagger \mathbf{F}^\top \mathbf{W}_Y \mathbf{F}, \quad (13)$$

where \mathbf{W} is the matrix of cotangent weights (6) and \dagger denotes the Moore-Penrose pseudoinverse.[‡] We stress that if \mathbf{F} is constructed in an intrinsic way, both shape difference operators $\mathbf{V}_{X,Y}$ and $\mathbf{R}_{X,Y}$ are intrinsic, since matrices \mathbf{A} and \mathbf{W} are expressed only in terms of edge lengths.

3.6. Shape analogies

Rustamov et al. [ROA*13] employed the shape difference operators framework to study shape analogies. Let A and B be shapes related by a functional map \mathbf{F} , giving rise to the shape difference operator $\mathbf{D}_{A,B}$ (area-based, conformal, or both), and let C be another shape related to A by a functional map \mathbf{G} . Then, one would like to know what would shape X be such that the difference $\mathbf{D}_{C,X}$ is equal to $\mathbf{D}_{A,B}$ under the functional map \mathbf{G} ? In other words, one wants to find an *analogy* of the difference between A and B (see Figure 1). To find such analogies, Rustamov et al. [ROA*13] considered a finite collection of shapes X_1, \dots, X_K and picked the shape minimizing the energy

$$\begin{aligned} X^* = \underset{X \in \{X_1, \dots, X_K\}}{\operatorname{argmin}} \quad & \| \mathbf{V}_{C,X} \mathbf{G} - \mathbf{G} \mathbf{V}_{A,B} \|_{\mathbb{F}}^2 \\ & + \| \mathbf{R}_{C,X} \mathbf{G} - \mathbf{G} \mathbf{R}_{A,B} \|_{\mathbb{F}}^2. \end{aligned} \quad (14)$$

The important question how to *generate* X from the given difference operator (rather than browsing through a collection of shapes) was left open.

4. Shape-from-Operator

We consider the *shape-from-operator* (SfO) problem: find an embedding \mathbf{X} of the shape, such that the discrete metric

[‡] Note that while the matrix \mathbf{A} is invertible, \mathbf{W} is rank-deficient (it has one zero eigenvalue) and thus is only pseudo-invertible.

$\ell(\mathbf{X})$ it induces would make an intrinsic operator (Laplacian, shape difference operator, etc.) satisfy some property or a set of properties (e.g., be as close as possible to some ‘reference’ operator). We consider a few examples of the SfO problem below.

Shape-from-Laplacian is a particular setting of the SfO problem, where one is given a pair of meshes X, Y related by the functional map \mathbf{F} . The embedding of Y is not given, but instead, we are given its stiffness matrix \mathbf{W}_Y (‘reference Laplacian’). The goal is to find an embedding \mathbf{X} that induces a Laplacian $\mathbf{W}(\ell(\mathbf{X}))$ as close as possible to \mathbf{W}_Y under the functional map \mathbf{F} , by minimizing

$$\mathcal{E}_{\text{lap}}(\mathbf{X}) = \|\mathbf{F}\mathbf{W}(\ell(\mathbf{X})) - \mathbf{W}_Y\mathbf{F}\|_{\text{F}}^2. \quad (15)$$

Note that our shape-from-Laplacian problem is different from the metric-from-Laplacian problems considered by [ZGLG12] and [dGMMD14] in the sense that we are additionally looking for an embedding that realizes the discrete metric. Secondly, unlike [ZGLG12, dGMMD14], we allow for arbitrary (not necessarily bijective) correspondence between X and Y .

Since the embedding minimizing (15) is defined up to isometry (rotation, translation, and also non-rigid deformation preserving edge lengths), the solution is not unique. Therefore, initialization has an important influence on the outcome: we are trying to deform some initial X such that its Laplacian is as close as possible to the given reference Laplacian. Since the Laplacian captures the intrinsic structure of the shape, the result of such optimization will be a shape in the initial pose of X but with the structure of Y , thus acting as a ‘style transfer’ (see Figure 1, center).

Shape-from-eigenvectors is a problem in which we are given a set of $r < n$ orthogonal vectors $\mathbf{U} = (\mathbf{v}_1, \dots, \mathbf{v}_r)$ on $L^2(X)$ and corresponding scalars $\Lambda = \text{diag}(\lambda_1, \dots, \lambda_r)$ and try to find an embedding \mathbf{X} inducing a Laplacian $\mathbf{W}(\ell(\mathbf{X}))$ that has eigenvectors \mathbf{U} and eigenvalues Λ ,

$$\begin{aligned} \mathcal{E}_{\text{evec}}(\mathbf{X}) = & \|\mathbf{W}(\ell(\mathbf{X}))\mathbf{U} - \mathbf{A}(\ell(\mathbf{X}))\mathbf{U}\Lambda\|_{\text{F}}^2 \\ & + \mu\|\ell(\mathbf{X}) - \ell_0\|_2. \end{aligned} \quad (16)$$

Here ℓ_0 denotes the discrete metric of the initial shape, and the last term acts as a regularization since the problem is ambiguous (there may be infinitely many Laplacians diagonalized by \mathbf{U}). We are thus looking for the smallest deformation (in the sense of the change of the discrete metric) that would make the Laplacian diagonalized by \mathbf{U} . Taking \mathbf{U} to be the eigenvectors of the Laplacian of some shape Y , we can create an ‘intrinsic hybrid’ between X and Y (see Figure 1, right), using Laplacians to capture the intrinsic structure (“style”) of the respective shapes, and averaging them by requiring them to be jointly diagonalizable by \mathbf{U} . The choice of the particular eigenvectors would determine whether high- or low-frequency structures of Y will be applied to X .

A more compelling application is in the study of shape collections. Kovnatsky et al. [KBB*13] showed how to find

a common intrinsic structure of a collection of shapes by ‘averaging’ the eigenspaces of the respective Laplacians by means of a joint diagonalization process. However, it is not clear what shape would give rise to a Laplacian with such an ‘average’ eigenspace. Such a shape can be found by solving the shape-from-eigenvectors problem (16), where \mathbf{U} and Λ are taken as the joint eigenvectors and eigenvalues of several Laplacians.

Shape-from-difference operator is the problem of synthesizing the shape analogy mentioned in Section 3.6, where we try to find an embedding \mathbf{X} that would induce difference operator between C, X as similar as possible to that between A, B by minimizing

$$\begin{aligned} \mathcal{E}_{\text{dif}}(\mathbf{X}) = & \mu\|\mathbf{A}_C^{-1}\mathbf{F}^\top\mathbf{A}(\ell(\mathbf{X}))\mathbf{F}\mathbf{G} - \mathbf{G}\mathbf{V}_{A,B}\|_{\text{F}}^2 \\ & + (1-\mu)\|\mathbf{W}_C^\dagger\mathbf{F}^\top\mathbf{W}(\ell(\mathbf{X}))\mathbf{F}\mathbf{G} - \mathbf{G}\mathbf{R}_{A,B}\|_{\text{F}}^2. \end{aligned} \quad (17)$$

Problem (17) is a version of (14) where instead of a search over a finite database of given shapes, one performs continuous optimization over the shape embedding. Problem (17) can be simplified if we choose the initial X to have a trivial correspondence with C ($\mathbf{F} = \mathbf{I}$), for instance, initializing $X = C$. In this case, we have simpler expressions for $\mathbf{V}_{C,X}(\mathbf{X}) = \mathbf{A}_C^{-1}\mathbf{A}(\ell(\mathbf{X}))$ and $\mathbf{R}_{C,X} = \mathbf{W}_C^\dagger\mathbf{W}(\ell(\mathbf{X}))$ leading to a simpler energy

$$\begin{aligned} \mathcal{E}_{\text{dif}}(\mathbf{X}) = & \mu\|\mathbf{A}_C^{-1}\mathbf{A}(\ell(\mathbf{X}))\mathbf{G} - \mathbf{G}\mathbf{V}_{A,B}\|_{\text{F}}^2 \\ & + (1-\mu)\|\mathbf{W}_C^\dagger\mathbf{W}(\ell(\mathbf{X}))\mathbf{G} - \mathbf{G}\mathbf{R}_{A,B}\|_{\text{F}}^2. \end{aligned} \quad (18)$$

Finally, if the shapes A, B have a bijective vertex-wise correspondence, the problem simplifies further since $\mathbf{G} = \mathbf{I}$.

4.1. Numerical optimization

All the aforementioned instances of the SfO problem have a two-level dependence (\mathbf{W} or \mathbf{A} depending on ℓ , which in turn depends on the embedding \mathbf{X}), making the optimization directly with respect to the embedding coordinates \mathbf{X} extremely hard. Instead, we split the problem into two stages: minimizing \mathcal{E} with respect to the discrete metric ℓ (*metric-from-operator* or MfO), and recovering the embedding \mathbf{X} from the metric ℓ (*shape-from-metric* or SfM).

Shape-from-metric (SfM) is well-known problem in geometry. Here, we address it as a special setting of the *multidimensional scaling* (MDS) problem [BG05] given a metric ℓ , find its Euclidean realization by minimizing the *stress*

$$\mathbf{Z}^* = \underset{\mathbf{X} \in \mathbb{R}^{n \times 3}}{\operatorname{argmin}} \sum_{i>j} v_{ij} (\|\mathbf{x}_i - \mathbf{x}_j\| - \ell_{ij})^2,$$

where $v_{ij} = 1$ if $ij \in E$ and zero otherwise. A classical approach for solving (19) is the iterative SMACOF Algorithm 1 [Lee77] based on the fixed-point iteration of the form $\mathbf{X} \leftarrow \mathbf{Z}^\dagger \mathbf{B}(\mathbf{X}) \mathbf{X}$, where

$$\mathbf{Z} = \begin{cases} -v_{ij} & i \neq j \\ \sum_{j \neq i} v_{ij} & i = j, \end{cases} \quad \mathbf{B}(\mathbf{X}) = \begin{cases} -\frac{v_{ij}\ell_{ij}}{\|\mathbf{x}_i - \mathbf{x}_j\|} & i \neq j \\ -\sum_{j \neq i} b_{ij} & i = j \end{cases} \quad (19)$$

are $n \times n$ matrices. Such iteration is guaranteed to produce a non-increasing sequence of stress values [BG05]. The matrix \mathbf{Z} is the combinatorial Laplacian, it depends only on the mesh connectivity and its pseudo-inverse \mathbf{Z}^\dagger is pre-computed.

Algorithm 1 SMACOF algorithm for SfM recovery.

Inputs: metric ℓ , initial embedding \mathbf{X}_0

Output: embedding \mathbf{X}

- 1: Initialize $\mathbf{X} \leftarrow \mathbf{X}_0$
 - 2: **for** $k = 1, \dots, N_{\text{MDS}}$ **do**
 - 3: $\mathbf{X} \leftarrow \mathbf{Z}^\dagger \mathbf{B}(\mathbf{X}) \mathbf{X}$,
 - 4: **end for**
-

Metric-from-operator (MfO) is the problem

$$\ell = \underset{\ell \in \mathbb{R}^{|E|}}{\operatorname{argmin}} \mathcal{E}(\ell) \quad \text{s.t. } (3), \quad (20)$$

where we have to restrict the search to all the valid discrete metrics satisfying the triangle inequality (3). In our experiments, optimization (20) was performed using the primal-dual interior-point algorithm implemented in the software package IPOPT [WB06], exploring second-order information (Hessian). This method is known to converge well even with non-convex cost functions. A filter line-search method is adopted by IPOPT, thus the Hessian of the Lagrangian function projected onto the null space of the constraint Jacobian needs to be positive-definite to guarantee certain descent properties of the filter line-search approach. These conditions are satisfied if the iteration matrix has exactly n positive, m negative, and no zero eigenvalues. For this purpose, the diagonal of the iteration matrix is perturbed by a small amount until the inertial is as desired. We refer to [WB06] for the relevant details.

Optimality The MfO problem is non-convex in general and hence theoretically liable to local convergence. However, as shown in the next section, we observed global convergence even in cases when the initialization was very far from the solution, so in practice this problem is well-behaved. The SfM problem is also non-convex, and furthermore, is largely ambiguous, as its minimizer is defined up to an isometry (rotation, translation, or more generally, length-preserving deformation). Therefore, we are interested in a *local minimizer* in the basin of attraction of the initial shape, and thus the choice of the initialization is important. Fortunately, in all our problems a simple and meaningful initialization is readily available: for example, in the shape-from-difference problem, it is natural to initialize $X = C$, and in the shape-from-Laplacian problem, the choice of the initialization determines the “pose” of the outcome.

5. Results

In this section, we show the applications of our approach for shape synthesis from intrinsic operators, considering the shape-from-Laplacian, shape-from-eigenvectors, and shape-from-difference operator problems described in Section 4.

For our experiments, we used shapes from standard shape collections including AIM@SHAPE, TOSCA [BBK08], and FAUST [BRLB14] resampled to 2K–5K vertices as well as additional synthetic shapes. Functional correspondences were computed according to (10) using k first Laplacian eigenfunctions and known vertex-wise correspondences as \mathbf{P}, \mathbf{S} .

5.1. Numerical properties of the problem

Complexity The complexity of our problem was evaluated in the shape-from-Laplacian setting (other settings have a similar structure and behave similarly), for shapes of increasing sizes, under the full correspondence assumption. The MfO subproblem was terminated when the gradient norm reached 10^{-11} . The SfM subproblem was solved using 100 iterations of SMACOF. Table 1 summarizes the breakdown of the run time.

	$ V $	$ E $	MfO		SfM	
			iters	time/ iter	time/ iter	total time
Sphere-Cylinder	182	540	14	0.07	1.9×10^{-3}	1.2
Sphere-Bump	642	1920	11	0.22	5.7×10^{-3}	3.0
Man-Gorilla	2470	7404	40	1.31	2.1×10^{-2}	54.4
Man-Fatman	3040	9114	144	1.57	2.7×10^{-2}	228.3
Man-Muscleman	5122	15360	87	3.36	4.2×10^{-3}	293.4

Table 1: Computational complexity (time in sec) of the MfO and SfM sub-problems of shape-from-Laplacian as a function of the number of vertices $|V|$ and edges $|E|$.

Convergence and sensitivity to initialization Figure 3 shows a typical convergence example of the MfO subproblem in shape-from-difference reconstruction problem (18). Optimization steps are visualized in Figure 10 (top). Figure 4 (top) shows convergence of the shape-from-Laplacian problem (15) with different initializations. Our optimization converges even if initialized by a shape very distant from the solution, and is not sensitive to bad meshing. As an experimental evidence of global convergence, in Figure 4 (bottom) we show that the distance from the metric of the reference shape converges to zero. An example of shape-from-Laplacian optimization intermediate steps is shown in Figure 7 (top).

Sensitivity to map quality Rustamov et al. [ROA*13] remark that “the quality of the information one gets from [shape difference operators] depends on the quality and density of the shape maps”. To illustrate this sensitivity, we show the result of shape-from-Laplacian reconstruction varying the quality of the functional map \mathbf{F} between X and Y (Figure 5), and the result of shape-from-difference operator reconstruction varying the quality of both functional maps \mathbf{F} between A, B and \mathbf{G} between A, C (Figure 6). In our experiment, the quality of the map is controlled by the number of the basis functions k used in the expansion (9). We can conclude that the output of our optimization is good as long as the functional maps are sufficiently accurate, and deteriorates when the map becomes too rough.

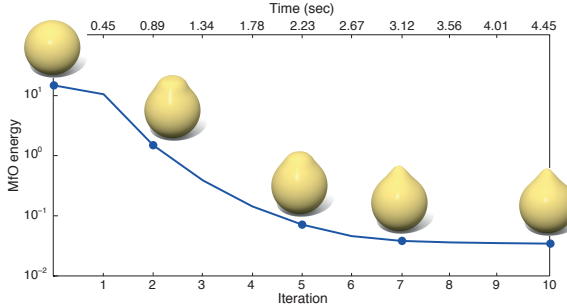


Figure 3: Convergence of the MfO subproblem in the shape-from-difference problem on shapes shown in Figure 1 (left).

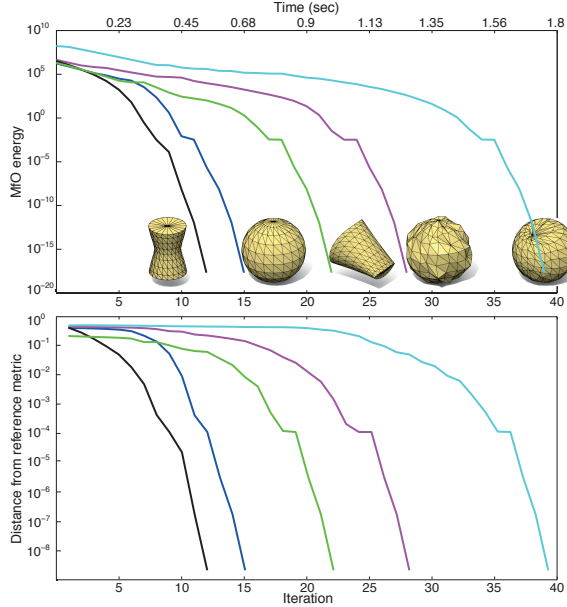


Figure 4: Convergence of the MfO subproblem in the shape-from-Laplacian problem for different initial shapes: shown is the MfO energy \mathcal{E}_{lap} (top) and distance from reference metric $\|\ell - \ell_0\|_2$ (bottom). The reference metric/Laplacian is taken from the cylinder shape.

5.2. Examples and applications

Shape-from-Laplacian reconstruction examples are shown in Figures 7 and 1 (center). In most experiments, we observed very fast convergence (order of tens of iterations) of the MfO sub-problem. Our method is able to cope with significantly different shapes such as man and gorilla. Because of the problem ambiguity (the solution is defined up to isometry), the choice of the initial shape defines the ‘pose’ of the shape, which is then deformed during the optimization process by transferring the ‘style’ (intrinsic structure captured by the Laplacian) from the reference shape.

Shape-from-eigenvectors We used the coupled diagonalization method of Kovnatsky et al. [KBB^{*}13] to compute 1000 joint approximate eigenvectors of the Laplacians of the

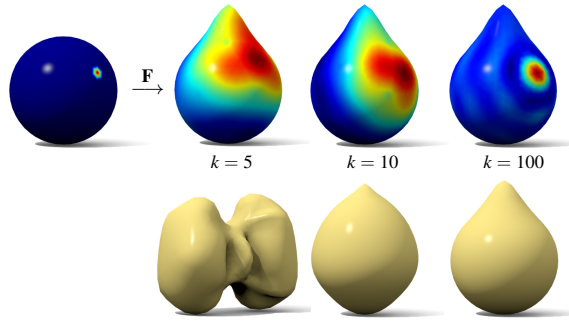


Figure 5: Dependence of the shape-from-Laplacian result on the quality of the functional maps. Top: functional maps of progressively improving quality (shown is the map of the function on the leftmost shape). Bottom: reconstruction results using sphere as initialization and reference Laplacian from bumped sphere.

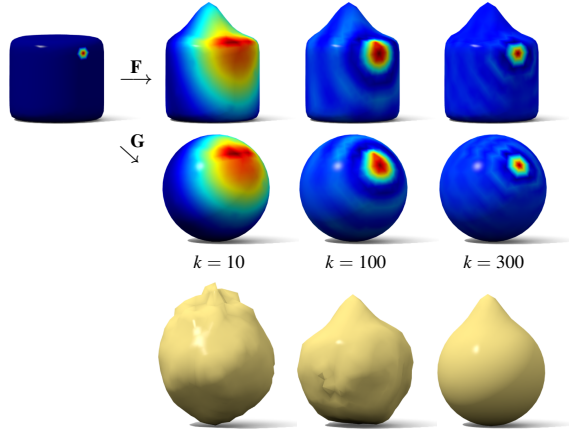


Figure 6: Dependence of the shape-from-difference operator result on the quality of the functional maps. Top: functional maps of progressively improving quality (shown is the map of the function on the leftmost shape). Bottom: shape analogy synthesis using sphere as initialization.

woman and fat man shapes in Figure 8 (top, two leftmost shapes). Then, the initial man shape (Figure 8, top third column) was deformed to have its Laplacian diagonalized by the joint eigenvectors Figure 8, bottom), resulting in an ‘intrinsic hybrid’ shape.

Shape-from-difference operator problem (18) was solved using $\mu = 1$ and initialized with $X = C$. Synthesized shapes are shown in Figures 10 and 1 (left). We observe that our method correctly transfers intrinsic shape differences and can cope with significantly different shapes such as thin and fat men, or human and alien. A particular setting when A has the same intrinsic geometry as B but is in a different pose (Figure 10, two bottom right examples) acts as a style transfer similar to shape-from-Laplacian.

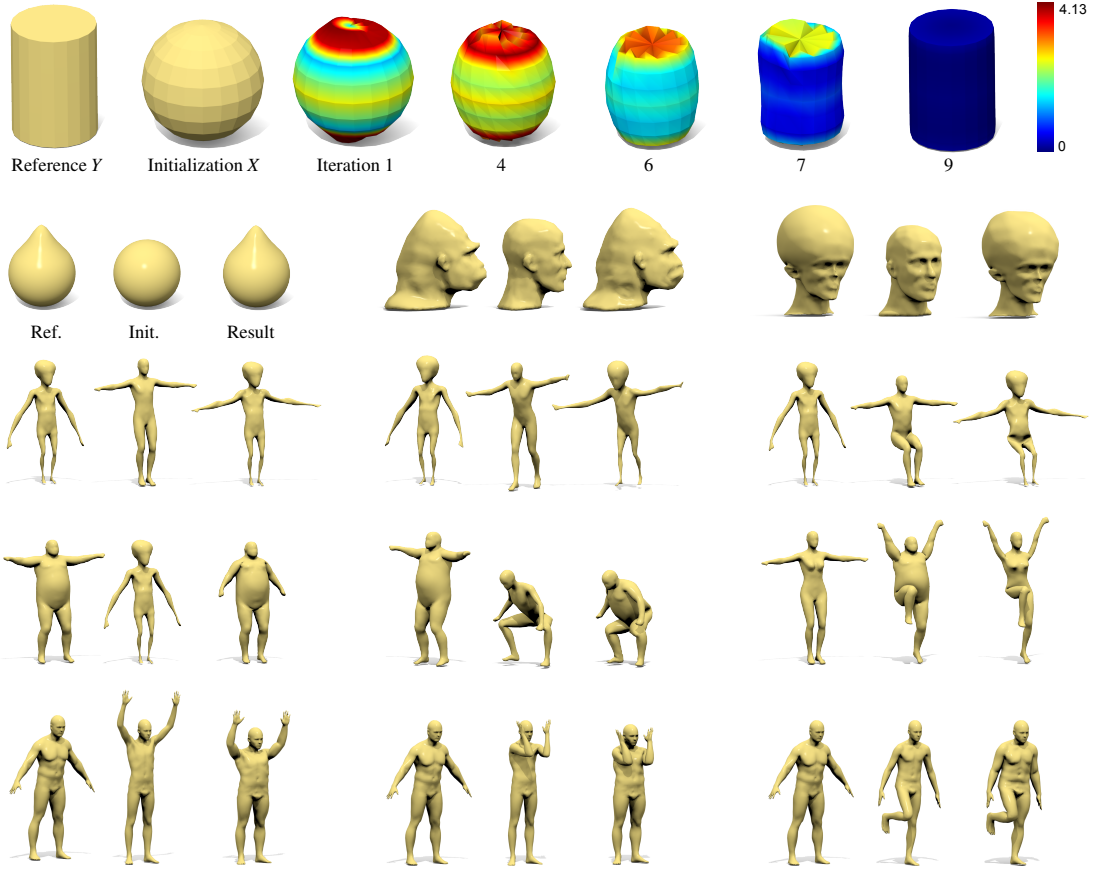


Figure 7: Shape-from-Laplacian. Top (left to right): shape used to compute reference Laplacian \mathbf{W}_Y , initial shape X , solution after a few MfO iterations. Colors show the vertex-wise MfO energy (computed as the sum of the edge-wise contribution to the energy for all edges shared by the vertex). Bottom: additional examples of shape-from-Laplacian reconstruction. Each column shows (left to right): reference, initial shape, result.

Shape exaggeration is an interesting setting of the shape-from-difference operator problem where $B = C$. In this case, the shape difference between A and B is applied to B itself, ‘caricaturizing’ this difference. Repeating the process several times, an even stronger effect is obtained (Figure 9).

6. Conclusions, limitations, and future work

We presented a framework for reconstructing shapes from intrinsic operators, showing as particular examples the problems of shape-from-difference operator, shape-from-Laplacian, and shape-from-eigenvectors. Our approach is readily extendable to other intrinsic operators. While the use of functional maps allows working with meshes with different number of vertices and triangulation, the sensitivity to the quality of the correspondence could be a factor limiting the application of our method. Another limitation is that our optimization does not allow to change the topology of the initial shape during the optimization.

In future works, we will explore reconstruction from additional intrinsic operators. An interesting future direction is to

consider shapes in different representation, such as meshes (with cotangent Laplacians) and point clouds (with graph Laplacians). Finally, we will study the use of other ways of reconstructing embedding from metric in place of MDS.

Acknowledgement

We are grateful to Fernando de Goes, Xianfeng Gu, Maks Ovsjanikov and Raif Rustamov for insightful comments. This work was supported by the ERC Starting Grant No. 307047.

References

- [ABCCO13] AZENCOT O., BEN-CHEN M., CHAZAL F., OVSJANIKOV M.: An operator approach to tangent vector field processing. *CGF* 32, 5 (2013), 73–82. [2](#)
- [ALX*14] ALHASHIM I., LI H., XU K., CAO J., MA R., ZHANG H.: Topology-varying 3D shape creation via structural blending. *TOG* 33, 4 (2014). [2](#)
- [BBK08] BRONSTEIN A. M., BRONSTEIN M. M., KIMMEL R.: *Numerical Geometry of Non-Rigid Shapes*. Springer, 2008. [6](#)
- [BCGB08] BEN-CHEN M., GOTSMAN C., BUNIN G.: Conformal flattening by curvature prescription and metric scaling. *CGF* 27, 2 (2008), 449–458. [2](#)

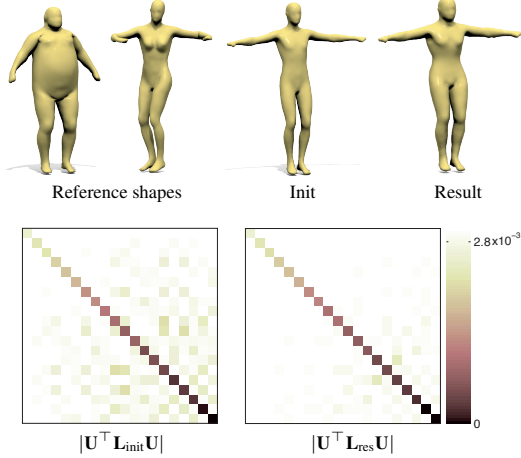


Figure 8: Shape-from-eigenvectors. Top (left-to-right): two shapes used to compute joint Laplacian eigenvectors \mathbf{U} ; initial shape, resulting hybrid shape. Bottom: diagonalization of the Laplacian by \mathbf{U} before (left) and after (right) optimization (only first 20 eigenvectors are shown).

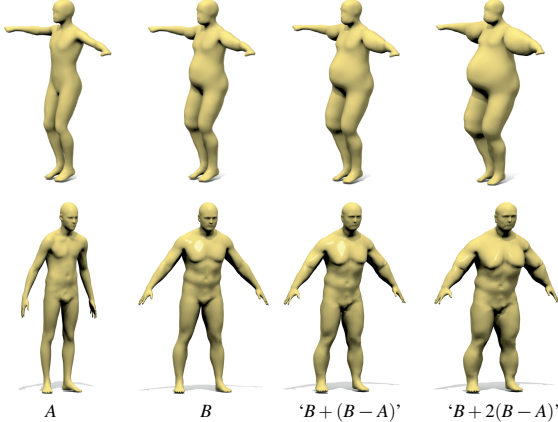


Figure 9: Shape exaggeration obtained by applying the difference operator between A, B to B several times.

- [BG05] BORG I., GROENEN P. J.: *Modern multidimensional scaling: Theory and applications*. Springer, 2005. 2, 5, 6
- [BGL13] BRONSTEIN M. M., GLASHOFF K., LORING T. A.: Making Laplacians commute. *arXiv:1307.6549* (2013). 2
- [BO00] BOHAN A., O'DONOGHUE D.: LUDI: A model for geometric analogies using attribute matching. In *Proc. AICS* (2000). 1
- [BRLB14] BOGO F., ROMERO J., LOPER M., BLACK M. J.: FAUST: Dataset and evaluation for 3D mesh registration. In *Proc. CVPR* (2014). 6
- [BVGPO9] BARAN I., VLASIC D., GRINSPUN E., POPOVIĆ J.: Semantic deformation transfer. *TOG* 28, 3 (2009), 36. 2
- [CCM11] CLARKE L., CHEN M., MORA B.: Automatic generation of 3D caricatures based on artistic deformation styles. *TVCG* 17, 6 (June 2011), 808–821. 2
- [CPS11] CRANE K., PINKALL U., SCHRÖDER P.: Spin transformations of discrete surfaces. *TOG* 30, 4 (2011), 104. 2
- [dGMMD14] DE GOES F., MEMARI P., MULLEN P., DESBRUN M.: Weighted triangulation for geometry processing. *TOG* (2014). 2, 4, 5
- [EKMB14] EYNARD D., KOVNATSKY A., M BRONSTEIN M.: Laplacian colormaps: a framework for structure-preserving color transformations. *CGF* 33, 2 (2014), 215–224. 2
- [HJO*01] HERTZMANN A., JACOBS C. E., OLIVER N., CURLESS B., SALESIN D. H.: Image analogies. In *Proc. Computer Graphics and Interactive Techniques* (2001). 2
- [IGG01] ISENBURG M., GUMHOLD S., GOTSMAN C.: Connectivity shapes. In *Proc. Visualization* (2001). 2
- [IH81] IKEUCHI K., HORN B. K. P.: Numerical shape from shading and occluding boundaries. *Artificial Intelligence* 17, 1-3 (1981), 141–184. 2
- [Ike84] IKEUCHI K.: Shape from regular patterns. *Artificial Intelligence* 22, 1 (1984), 49 – 75. 2
- [JS12] JACOBSON A., SORKINE O.: *A Cotangent Laplacian for Images as Surfaces*. Tech. Rep. 757, ETH Zurich, 2012. 3
- [Kan85] KANATANI K.-I.: Structure from motion without correspondence: General principle. In *Proc. IJCAI* (1985). 2
- [KBB*13] KOVNATSKY A., BRONSTEIN M. M., BRONSTEIN A. M., GLASHOFF K., KIMMEL R.: Coupled quasi-harmonic bases. *CGF* 32 (2013), 439–448. 5, 7
- [KG08] KIRCHER S., GARLAND M.: Free-form motion processing. *TOG* 27, 2 (2008), 12. 2
- [KH06] KARPENKO O. A., HUGHES J. F.: Smoothsketch: 3D free-form shapes from complex sketches. *TOG* 25, 3 (2006), 589–598. 2
- [LBB11] LITMAN R., BRONSTEIN A. M., BRONSTEIN M. M.: Diffusion-geometric maximally stable component detection in deformable shapes. *Computers & Graphics* 35, 3 (2011), 549–560. 4
- [Lee77] LEEUW J. D.: Applications of convex analysis to multidimensional scaling. In *Recent Developments in Statistics* (1977), pp. 133–146. 5
- [LSLC05] LIPMAN Y., SORKINE O., LEVIN D., COHEN-OR D.: Linear rotation-invariant coordinates for meshes. *TOG* 24, 3 (2005), 479–487. 2
- [LVM*11] LEWINER T., VIEIRA T., MARTÍNEZ D., PEIXOTO A., MELLO V., VELHO L.: Interactive 3D caricature from harmonic exaggeration. *Computers & Graphics* 35, 3 (2011), 586–595. 2
- [MDSB03] MEYER M., DESBRUN M., SCHRÖDER P., BARR A. H.: Discrete differential-geometry operators for triangulated 2-manifolds. *Visualization&Mathematics* (2003), 35–57. 3
- [MHS*14] MA C., HUANG H., SHEFFER A., KALOGERAKIS E., WANG R.: Analogy-Driven 3D Style Transfer. *CGF* 33, 2 (2014), 175–184. 2
- [MWZ*13] MITRA N., WAND M., ZHANG H. R., COHEN-OR D., KIM V., HUANG Q.-X.: Structure-aware shape processing. In *SIGGRAPH Asia 2013 Courses* (2013). 2
- [OBCS*12] OVSJANIKOV M., BEN-CHEN M., SOLOMON J., BUTSCHER A., GUIBAS L.: Functional maps: A flexible representation of maps between shapes. *TOG* 31, 4 (2012). 2, 4
- [PP93] PINKALL U., POLTHIER K.: Computing discrete minimal surfaces and their conjugates. *Experimental Mathematics* 2, 1 (1993), 15–36. 3
- [PPTSH14] PANIZZO D., PUPPO E., TARINI M., SORKINE-HORNUNG O.: Frame fields: Anisotropic and non-orthogonal cross fields. *TOG* 33, 4 (2014), 134. 2

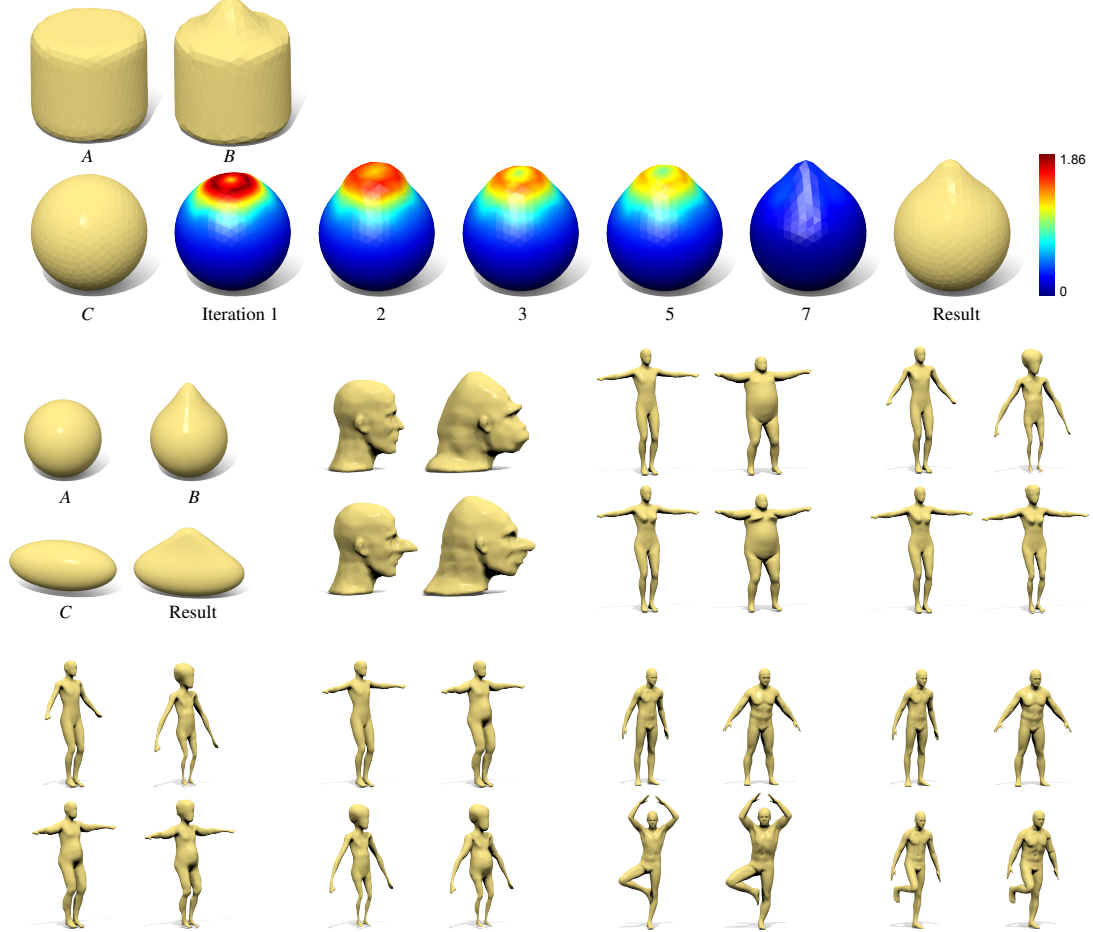


Figure 10: Shape analogy synthesis by solving the shape-from-difference operator problem. Top: solution a after a few MfO iterations (colors show the vertex-wise MfO energy). Bottom: additional examples of shape analogies synthesized with our approach.

- [RCG08] RONG G., CAO Y., GUO X.: Spectral mesh deformation. *Visual Computer* 24, 7 (2008), 787–796. [2](#)
- [ROA*13] RUSTAMOV R. M., OVSJANIKOV M., AZENCOT O., BEN-CHEN M., CHAZAL F., GUIBAS L.: Map-based exploration of intrinsic shape differences and variability. *TOG* 32, 4 (2013), 1–12. [1](#), [2](#), [4](#), [6](#)
- [Ros97] ROSENBERG S.: *The Laplacian on a Riemannian manifold: an introduction to analysis on manifolds*. Cambridge University Press, 1997. [2](#)
- [SCOL*04] SORKINE O., COHEN-OR D., LIPMAN Y., ALEXA M., RÖSSL C., SEIDEL H.-P.: Laplacian surface editing. In *Proc. SGP* (2004). [2](#)
- [SdS01] SHEFFER A., DE STURLER E.: Parameterization of faceted surfaces for meshing using angle-based flattening. *Engineering with Computers* 17, 3 (2001), 326–337. [2](#)
- [SOG09] SUN J., OVSJANIKOV M., GUIBAS L.: A concise and provably informative multi-scale signature based on heat diffusion. *CGF* 28, 5 (2009), 1383–1392. [4](#)
- [SP04] SUMNER R. W., POPOVIĆ J.: Deformation transfer for triangle meshes. *TOG* 23, 3 (2004), 399–405. [2](#)
- [WB06] WÄCHTER A., BIEGLER L. T.: On the implementation of an interior-point filter line-search algorithm for large-scale nonlinear programming. *Mathematical Programming* 106, 1 (2006), 25–57. [6](#)
- [WBAL11] WELNICKA K., BÆRENTZEN J., AANÆS H., LARSEN R.: *Descriptor Based Classification of Shapes in Terms of Style and Function*. Tech. rep., IMM, 2011. [2](#)
- [Wit80] WITKIN A. P.: *Shape from contour*. PhD thesis, MIT, 1980. [2](#)
- [WLT12] WANG Y., LIU B., TONG Y.: Linear surface reconstruction from discrete fundamental forms on triangle meshes. *CGF* 31, 8 (2012), 2277–2287. [2](#)
- [Woo80] WOODHAM R. J.: Photometric method for determining surface orientation from multiple images. *Optical Engineering* 19, 1 (1980), 139–144. [2](#)
- [XLZ*10] XU K., LI H., ZHANG H., COHEN-OR D., XIONG Y., CHENG Z.-Q.: Style-content separation by anisotropic part scales. *TOG* 29, 6 (2010), 184. [2](#)
- [ZGLG12] ZENG W., GUO R., LUO F., GU X.: Discrete heat kernel determines discrete Riemannian metric. *Graphical Models* 74, 4 (2012), 121–129. [2](#), [3](#), [5](#)